Phase boundaries and critical and tricritical properties of monolayer ^{4}He adsorbed on graphite

R. E. Ecke,* Q.-S. Shu,† T. S. Sullivan, and O. E. Vilches
Department of Physics, University of Washington, Seattle, Washington 98195
(Received 9 July 1984)

We report heat-capacity measurements on ^{4}He films adsorbed on graphite for surface densities at and smaller than that required to form a commensurate $(\sqrt{3}\times\sqrt{3})R30°$ monolayer in the temperature range 0.4 K $< T <$ 4.2 K. At densities below 0.039 Å^{-2}, a single transition is observed at $T < 1.3$ K. For densities larger than 0.039 Å^{-2}, two transitions are observed, the higher-T one developing into the order-disorder transition previously studied by several authors. Our measurements are consistent with a phase diagram showing a large region of existence of a single-phase commensurate (with vacancies) film, and a two-phase region of coexisting commensurate and vapor phases. For this phase diagram a tricritical point exists at $T_{TCP} \cong 1.3$ K and a density $n_{TCP} \simeq 0.039$ Å^{-2}. We observe strong evidence for Fisher renormalization of the constant-density specific heat along the critical line. The effects of inhomogeneities on all transitions are discussed.

I. INTRODUCTION

^{4}He adsorbed on the basal plane of exfoliated graphite provides an excellent system for the study of two-dimensional (2D) phase transitions. At intermediate densities, $n = 0.0637$ Å^{-2}, helium registers in the $(\sqrt{3}\times\sqrt{3})R30°$ structure.[1-3] The order-disorder transition from registered to fluid, which was shown to be in the same universality class as the three-state Potts model[4] and is marked by strongly divergent specific-heat peaks near 3 K, was first measured by Bretz *et al.*[1] for a Grafoil[5] substrate. Subsequent specific-heat measurements by Bretz[6] using a *ZYX* substrate yielded higher, sharper peaks characterized by a critical exponent $\alpha \cong 0.36$, close to the theoretical three-state Potts value of $\frac{1}{3}$.[7,8] Other specific-heat measurements on graphite foam[9,10] also yielded values of α close to $\frac{1}{3}$.

At low density, between 0.01 and 0.04 Å^{-2}, ^{4}He behaves like an imperfect quantum gas above about 2 K. Siddon and Schick[11] accounted for deviations from the 2D ideal-gas result of $C/Nk_B = 1$ by calculating the quantum second virial correction. Their calculation of the specific heat showed a divergence near 1.5 K. This is close to the temperature where there are rounded peaks in the experimental heat capacity, which suggested that the gas becomes unstable with respect to a condensed phase and that the peak is the signature of a phase transition. Further support for this idea was provided by Novaco,[12] who estimated the ground-state energy of gas, liquid, and registered phases and showed that the liquid has the lowest energy in the low-density regime. Although the registered structure was calculated to be energetically unfavorable, an increase in the substrate corrugation would favor the registered phases. Cole and co-workers[13] showed that the helium-graphite interaction potential is appreciably more corrugated than previous calculations[14] had indicated. Although the nature of the condensed phase was uncertain, the peaks in the constant-density heat capacity seemed to represent a transition from a vapor-condensed phase coexistence region at low temperature to a single-phase quantum gas at high temperatures. In an ideal system, the specific-heat signature due to crossing this boundary should be a discontinuity, but in the presently realizable systems the rounding of the experimental peaks can be explained as due to variations in substrate binding energy.[15,16]

The location of heat-capacity peaks on low-density ^{4}He/graphite from previous measurements is shown in Fig. 1. Several questions remained concerning the nature of the condensed phase and the location of the phase boundary of the registered phase. Several authors have presented possible phase diagrams based on calculations of the properties of lattice gas[17] and the three-state Potts lattice-gas model.[18] If the registered phase is preferred over the liquid as the ground state, then there must be a three-state Potts tricritical point where the critical region joins the two-phase coexistence region. The properties of

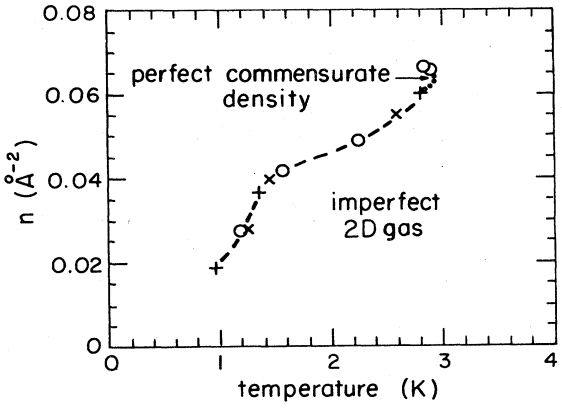

FIG. 1. Position of heat-capacity peaks from previous measurements for ^{4}He/graphite for densities at and below the perfect commensurate one. Type of graphite used in parentheses. Data of Bretz (Ref. 6) (*ZYX*) near n_c not included since they would be indistinguishable on the scale of drawing. ×, Bretz and Dash (Ref. 1) (Grafoil); ○, Hickernell *et al.* (Ref. 1) (Grafoil); +, Tejwani *et al.* (Ref. 9) (foam); ●, Ecke and Dash (Ref. 28) (foam).

the tricritical region should be described by scaling theory,[19–21] hence the helium data might provide a comparison with the predictions of the theory.

We have studied the region of ^{4}He adsorbed on graphite foam[5] between 0.0259 and 0.0662 Å^{-2} using adiabatic calorimetry and have delineated the two-phase coexistence region and the critical line. The condensed phase in the coexistence region is interpreted to be the registered phase. Although the exact location of the tricritical point has not been resolved in this study, we estimate it to occur at $T_{TCP} \cong 1.3$ K and $n_{TCP} \cong 0.039$ Å^{-2}. The results are consistent with the predictions of scaling theory.

Several years ago Elgin and Goodstein[22,23] did a complete thermodynamic analysis of the data existing up to that time for ^{4}He adsorbed on graphite. Their method was successfully used a few years later to calculate the binding energy for a single helium atom on graphite, using only thermodynamic methods.[24] Of particular importance to our work is the fact that in their original work they measured and calculated the chemical potential at many densities and temperatures. In addition they showed how to calculate the chemical potential at low temperatures given a set of initial values and an extensive measurement of the heat capacity of the system. We have used their method and some of their chemical-potential values to do a semiquantitative study of the critical and tricritical regions of the phase diagram. Along the critical line the constant-density specific-heat peaks show the beginning of crossover towards "Fisher-renormalized" exponents.[25] Although the renormalization region is obscured by finite size and heterogeneity effects, a reconstruction of the constant-chemical-potential specific heat produces a dramatic increase in peak height and sharpness over the constant density peaks.

II. EXPERIMENT AND DATA

The specific-heat data were obtained using the adiabatic technique described elsewhere.[1] The heat-capacity cell was an internally gold-plated thin-wall copper can enclosing 4.13 g of graphite foam which had been baked under vacuum at 900 °C for 4 h. The cell was suspended from the mixing chamber of a dilution refrigerator by a 2-in. nylon tube (wall thickness: 0.002 in.). The mixing chamber temperature could be varied from about 10 mK up to over 4 K by applying heat with an electrical heater. In this study, the range was 0.4 to 4 K. The temperature of the cell was measured with a Matsushita resistance thermometer which has a 4.2-K resistance of about 180 Ω. The carbon resistor was calibrated against a Cryo-Cal model CR50 germanium resistance thermometer which was factory calibrated above 1.5 K.[26] The calibration was extended between 0.1 and 1.5 K using a cerium magnesium nitrate susceptibility thermometer and an S.H.E. Corporation SQUID (Ref. 27) (superconducting quantum interference device) detector. The resistance of the carbon thermometer was calibrated for each run.

The heat-capacity data are estimated to be 1% accurate from 0.4 to 3.5 K but become increasingly more scattered between 3.5 and 4 K, due to decreasing resistor sensitivity and increasing thermal conductivity between the cell and mixing chamber and less accurate due to uncertainties in the resistance calibration.

TABLE I. ^{4}He coverages. V, gas volume adsorbed; N, number of atoms; n, surface density; $n_m = 0.115$ Å^{-2}, monolayer density.

V (STP cm^3)	N ($\times 10^{20}$)	n (Å^{-2})	n/n_m
9.79	2.628	0.025 91	0.225
13.01	3.493	0.034 44	0.299
13.94	3.742	0.036 90	0.321
16.03	4.303	0.042 43	0.369
18.53	4.977	0.049 07	0.427
21.65	5.813	0.057 32	0.498
22.42	6.022	0.059 37	0.516
22.75	6.108	0.060 23	0.524
23.26	6.247	0.061 60	0.536
23.66	6.352	0.062 63	0.545
24.04	6.457	0.063 67	0.554
25.00	6.713	0.066 19	0.576

Helium gas (nominal purity 99.99%) was introduced into the cell in doses (accurate to 0.2%) using a calibrated volume and two MKS Instruments, Inc. Baratron capacitive-pressure manometers. The film was annealed by heating the cell until the cell vapor pressure increased to between 10 and 50 mTorr. This pressure was maintained for a minimum of 3 h after which the cell cooled slowly back to 4 K. This procedure has been shown to produce well-annealed films for ^{4}He adsorbed on graphite foam.[28] No features were seen in our measurements which could be attributed to incomplete annealing of the film.

Specific-heat data were taken for twelve coverages, Table I, and for a background run with no adsorbed gas. Typical temperature increments for the heat-capacity data are 1% to 2% of the absolute temperature. The background heat-capacity points were fitted to a third-order polynomial and subtracted from the total heat capacity for each coverage to yield the film specific heat. The resultant signal to background ratio varied from 1/2 at the lowest coverage and high T, where $C/Nk_B \cong 1$ to 20/1 at the critical coverage, and close to T_c where $C/Nk_B \cong 8$. The surface area of the sample was deter-

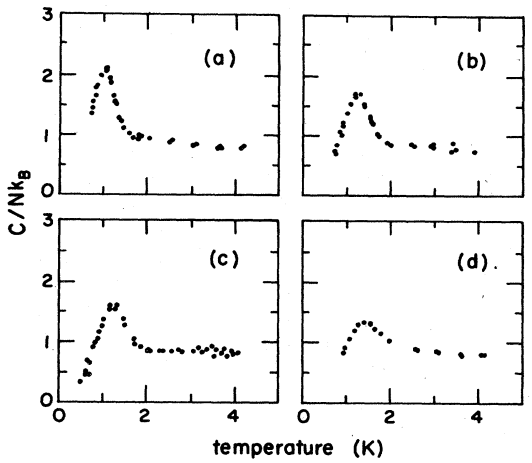

FIG. 2. Specific heat for ^{4}He/graphite foam. Coverages in Å^{-2} are (a) 0.0259, (b) 0.0344, (c) 0.0369, and (d) 0.0424.

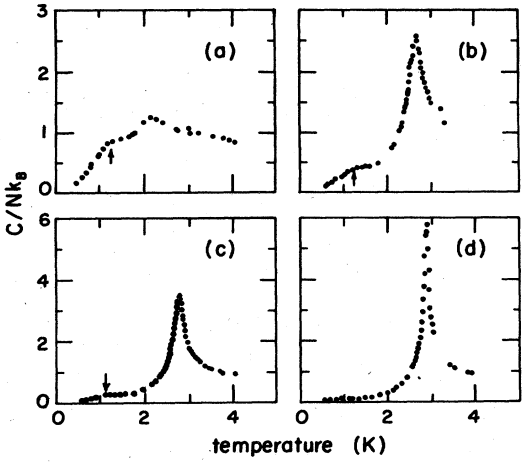

FIG. 3. Specific heat for ^{4}He/graphite foam. Coverages in Å^{-2} are (a) 0.0491, (b) 0.0573, (c) 0.0594, and (d) 0.0616.

mined by locating the critical coverage ($n_c = 0.063\,67$ Å^{-2}) using the standard method involving the specific-heat peak maxima.[1,26] The sample area is found to be 101.4 m^2 with a specific area of 24.6 m^2/g, somewhat smaller than values reported for other graphite-foam samples.[28,29]

III. RESULTS

The specific-heat data divide into two regimes. Below $n = 0.039$ Å^{-2} a single peak in the specific heat occurs. The peak shifts to higher temperature with increasing coverage, Fig. 2. All of these peaks have temperature widths similar to those found at comparable density in ^{4}He/Grafoil. At higher coverage, 0.039 Å$^{-2} < n < 0.063$ Å^{-2}, a rounded anomaly at $T < 1.3$ K and a higher-temperature peak appear, Fig. 3. The low-temperature anomaly decreases in amplitude and shifts slowly to lower temperature, Fig. 4, while the high-temperature peaks increase rapidly in magnitude and temperature as the density increases towards n_c, Fig. 5. The temperature width of the anomalies shown in Fig. 4 remains constant at about T (full width at half maximum) $= 0.4$ K.

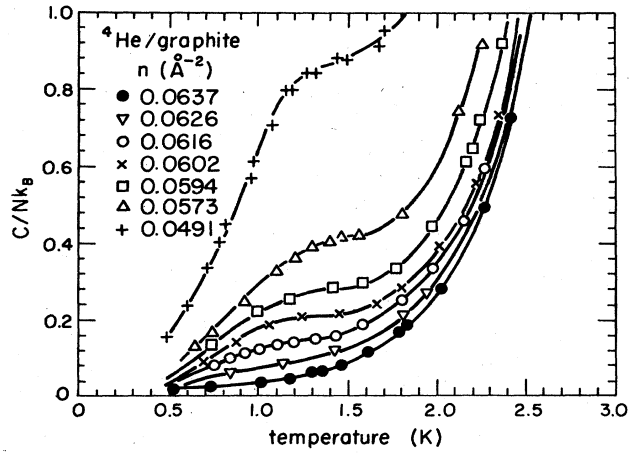

FIG. 4. Specific heat for ^{4}He/graphite foam at densities that show a low-temperature anomaly.

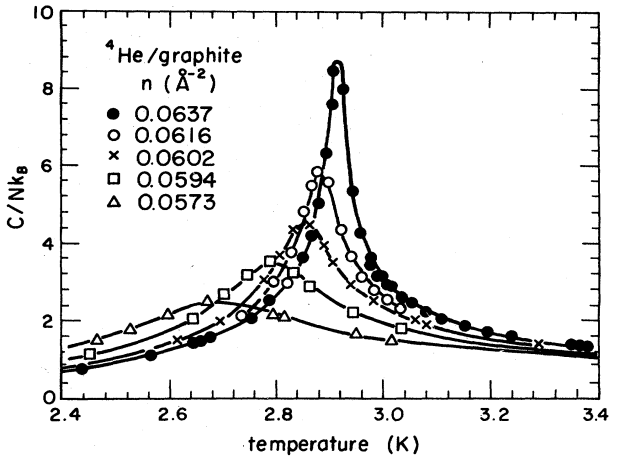

FIG. 5. Specific heat for ^{4}He/graphite foam at and below the critical density $n_c = 0.0637$ Å^{-2}.

IV. DISCUSSION

The data presented in the previous section were used to construct a tentative phase diagram based on identifying the peaks with the crossing of phase-boundary lines, Fig. 6. The error bars, particularly in the low-temperature boundary, represent the rounding of and the uncertainty in determining the peak maxima. Two points are plotted for $n = 0.0424$ Å^{-2} [see Fig. 2(d)]. The flattening of the peak top seems to be indicative of two superimposed peaks. The interpretation of the phase diagram presented in Fig. 6 is based on the belief that the phase transitions in the ^{4}He/graphite system are in the same universality class of the 2D three-state Potts model.

Close to the critical coverage (n_c) the identification of region II as the commensurate $(\sqrt{3}\times\sqrt{3})R30°$ phase is supported by specific-heat data[1,6,9] and neutron scattering data.[2,3] The commensurate-fluid transition at n_c is continuous. At lower density and low enough temperatures, it is expected that the long-range ordered commensurate

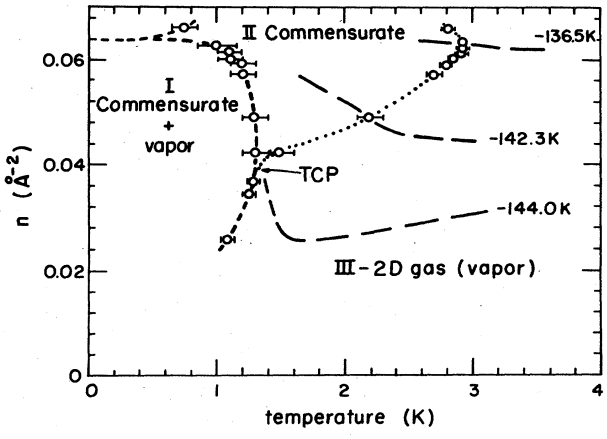

FIG. 6. Location of heat-capacity peaks and broad anomalies, and proposed phases and phase boundaries. · · · ·, critical line; — — —, two-phase line; ——, lines of constant chemical potential μ; values of μ/k_B are noted in the figure.

phase will break up into two phases, a commensurate phase and a low-density fluid (vapor) phase. The point in the (T,n) diagram where the continuum transition line (critical line) meets the two-phase region boundary is a tricritical point (TCP). While it is impossible to locate accurately the TCP from our data, scaling places certain restrictions on the phase boundary at the TCP for the three-state Potts model, namely, that the critical line should approach the two-phase boundary tangentially and that $(dT/dn)_{cr}=0$ at the TCP.[20] We have sketched in Fig. 7 the three possibilities consistent with this requirement.

In addition, the tricritical exponents of certain thermodynamic functions are specified by the three-state Potts model. The density difference between the two coexisting phases for $T<T_{TCP}$ should vary like

$$\Delta n \sim |t|^{\beta_T}, \tag{1}$$

where $t=(T-T_{TCP})/T_{TCP}$. The three-state Potts lattice-gas value for β_T is $\frac{1}{2}$. The property which we measure directly is the constant-density specific heat which should scale like

$$C_n \sim |t|^{3/2}, \tag{2}$$

at $n=n_{TCP}$ corresponding to a negative tricritical exponent, $\alpha_T=-\frac{3}{2}$. The constant-density specific heat given by (2) does not diverge (it will go to a constant value as $t\rightarrow 0$) and has a finite first derivative which indicates a rounded rather than cusp-shaped peak. Thus, unless the amplitude of the singular (temperature-dependent) part is large, the specific-heat signature of the TCP will be very hard to observe.

The observed signal in our measurement qualitatively agrees with the expectations above. As the density approaches $n\leq 0.039$ Å^{-2} from below, the specific-heat peaks become wider and of smaller magnitude until at that density one has the roundest and smallest peak. Thus our measurements point toward the TCP being in the vicinity of $n\cong 0.039$ Å^{-2} and $T\cong 1.3$ K and the phase diagram being like Fig. 7(c), rather than along the boundary between regions II and III shown in Fig. 6. In fairness, there are not enough different density runs to locate a possible inflection point along the II-III boundary [as in Fig. 7(b)], but the present specific-heat data substantially limit the amplitude of the inflection. Note that the third possibility that the TCP is located at n_c and $T_c=3.95$ K [as in Fig. 7(a)], where $(dT/dn)_{cr}=0$ is not realistic because of

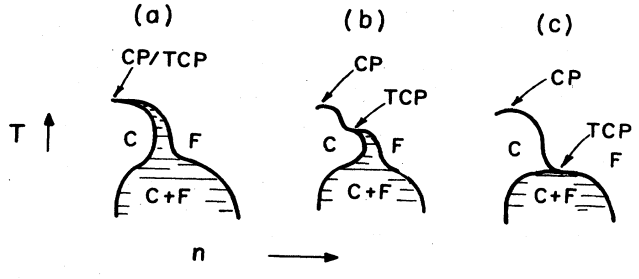

FIG. 7. Three possible T-n phase diagrams consistent with the 2D three-state Potts model. C, commensurate; F, fluid; CP, critical point; TCP, tricritical point.

the strong divergence of the specific heat at that density which reflects critical rather than tricritical behavior.

A potential problem with our interpretation is whether or not the low-temperature rounded anomalies for $n>0.04$ Å^{-2} actually represent the crossing of a phase boundary. Butler *et al.*[30] pointed out that in a two-phase region, a rounded peak in the heat capacity can be due to a rapidly changing phase-boundary slope. Subsequent experimental measurements by Migone *et al.*[31] confirmed this idea for N_2 adsorbed on graphite. However, an important restriction of the model of Butler *et al.* is that the resultant peak temperature must be greater than or equal to the temperature where the phase-boundary slope changes rapidly. Figure 4 shows that the peak temperature shifts to lower temperature as coverage is increased. Therefore the peaks are not caused by the phase-boundary mechanism and can be interpreted as actual phase-boundary anomalies rounded out by heterogeneities (see discussion below).

If the TCP is in the vicinity of $n\cong 0.039$ Å^{-2} and $T\cong 1.3$ K, a value of $\beta_T=0.4+0.2$, consistent with the theoretical predictions, can be obtained from the data. The large uncertainty in β_T comes from a reduced temperature range of only $0.05<|t|<0.25$ and the large uncertainties in the location of the TCP and the phase boundary.

The other phenomenon probed in this experiment is the behavior of the specific heat along the critical line (the phase boundary between regions II and III of Fig. 6). At the critical coverage n_c, specific-heat experiments of ^{4}He adsorbed on different exfoliated graphite substrates have yielded values of α close to the exact value for the 2D three-state Potts model of $\frac{1}{3}$. As the density decreases from n_c, the phase boundary moves to lower temperatures, and the specific-heat peak associated with the order-disorder transition decreases in magnitude. This has been observed in all previous experiments along the critical line and in the theoretical calculation of Ref. 15. We believe that the behavior of the measured specific heat is due to the fact that the measurements are being done at *constant density* and not at *constant chemical potential.* The registered phase exists over a range of densities because vacancies can exist without destroying the order of the phase. Since vacancies are irrelevant with respect to the critical behavior of the registered phase, the specific-heat divergence should be characterized by the same value of α along the critical line.[19] However, for a constant-density path the critical exponent α is renormalized to $\alpha_R=-\alpha/(1-\alpha)$ [except where $(dT/dn)_{cr}$, the slope of the critical line, is zero]. For the three-state Potts model then $\alpha_R=-\frac{1}{2}$. This means that $C_n\sim|t|^{-\alpha_R}=|t|^{1/2}$ will have a finite cusp singularity rather than the $|t|^{-\alpha}=|t|^{-1/3}$ divergence of C_μ. This effect (called Fisher renormalization) was first proposed independently on the basis of thermodynamic considerations by Fisher[25] and by Lipa and Buckingham.[32] Numerical calculations on three-dimensional (3D) Ising-type models have been performed by Fisher and Scesney[33] and by Riedel and Wegner.[34] Results of the calculations show that for $|t|$ values larger than a "crossover" temperature region C_μ and C_n have similar temperature dependences, while for

$|t|$ smaller than the crossover temperature region, C_n behaves like the renormalized specific heat. The crossover reduced temperature (t_{cr}) density dependence can be crudely estimated to behave, for small $x=(n-n_c/n_c)$, like $t_{cr}\sim x^{1/\alpha}$ near n_c. So the renormalized region goes to 0 as x goes to 0. For the 3D Ising models the fully renormalized region is not observed until very small values of $|t|$ ($\cong 10^{-5}$) are reached.[33,34] The larger value of α for the 2D three-state Potts system may lead to a larger range of $|t|$ where the fully renormalized behavior is observed. In the following discussion we present experimental evidence that the temperature dependence of the measured C_n is consistent with the expectations from critical exponent renormalization.

In Fig. 8 the specific-heat peaks for densities close to n_c are plotted on a single scale of reduced temperature. We use as T_c for each density the temperature of the peak determining the phase boundary. In Fig. 8 are traces of the data shown as a succession of peaks in Fig. 5. The most important observation in Fig. 8 is that for large enough $|t|$, all runs at $n<n_c$ fall exactly on top of each other. While the exact superposition is probably a coincidence we can use this fact to establish that in the range where $C_n=C_{n_c}$ the constant-density specific heat has the same reduced temperature behavior as the critical specific heat at the highest T_c in the phase boundary. Since this last one has been fitted by $\alpha\cong\frac{1}{3}$ and should not be renormalized, we conclude that in the region of superposition α(constant n)=α(constant μ). This region of superposition is shown in Fig. 9 between the dashed and dotted lines on each side of the phase boundary. The dotted line represents a range of $|t|=0.12$ to each side of the critical line. This is the range fitted by $\alpha\cong\frac{1}{3}$ in Bretz[6] and Tejwani *et al.*[9] measurements at n_c. For $|t|$ smaller than the region of superposition, the specific-heat magnitude is smaller the larger the deviation of n from n_c (larger x). This is the correct direction for going into renormalized behavior. Unfortunately the experimental system is not "perfect" in that rounding of the specific heat occurs even at n_c for the largest specific-heat peak. This rounding is due to heterogeneities (see below). The successive peaks along the critical line also show rounding at increasing values of $|t|$ as x increases. The inflection point on the specific-heat peaks has been taken as indicative of the rounding, and they delineate the heavy dashed lines of Fig. 9. The region between the two dashed lines on each side of the critical line should fall (at least) in the crossover region and data taken there could serve for comparison to theoretical models of crossover phenomena. If this is the case, an evaluation of C_μ within that region should give a diverging specific heat rather than the rounded C_n peaks observed. We have done a semiquantitative calculation with results shown in Fig. 10. It is obvious that one recovers a specific-heat peak of approximately the same peak height as the one found at n_c, while the peak of C_n is only $\frac{1}{3}$ the magnitude. The calculation was

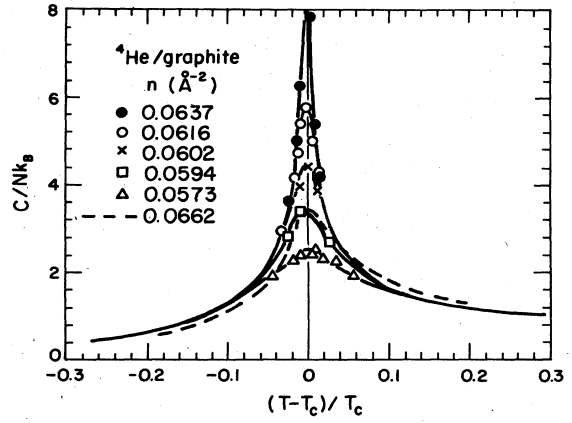

FIG. 8. The specific heat at and near n_c plotted as a function of reduced temperature. For each density, T_c has been taken as the temperature of the maximum specific heat. For clarity, experimental points are not plotted. Notice that the run taken with $n>n_c$ does not fall on top of the runs with $n<n_c$.

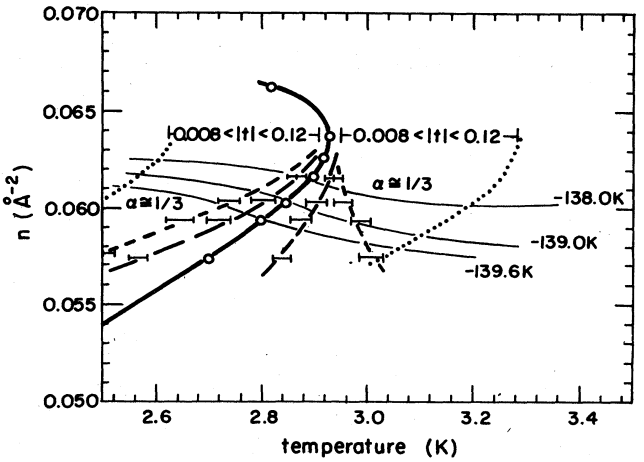

FIG. 9. The phase boundary near n_c and T_c, showing the regions where rounding, Fisher renormalization, and superposition (see text and Fig. 8) of the specific heat take place. The bar at n_c corresponds to the interval in $|t|$ where $\alpha\cong\frac{1}{3}$ in Ref. 9. Lines of constant μ/k_B calculated as described in text are indicated.

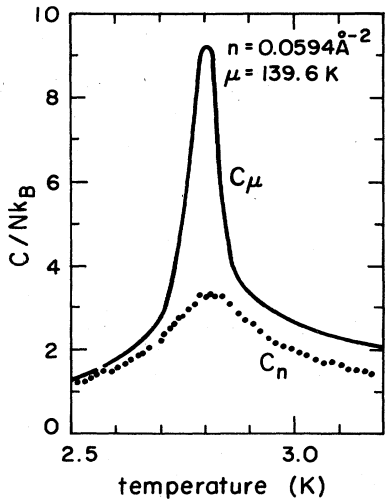

FIG. 10. Experimental C_n and calculated C_μ for constant-density and constant-chemical-potential paths that cross the critical line at $T=2.80$ K.

done by using a thermodynamic procedure described by Elgin and Goodstein[22] and Elgin,[23] as follows.

We calculated the chemical potential from our specific-heat data by numerical integration of $(dS/dN)_T = -(d\mu/dT)_N$. First we constructed an entropy-temperature-density table by integration of C_n/T from $T=0$. Our C_n data were extrapolated to $T=0$ K by using the same temperature dependence of C_n found by Hickernell *et al.*[35] who, using a Grafoil cell, obtained data at a few coverages to much lower temperature than that of this study. The temperature dependence well below the peaks was approximately $T^{2.2}$. This procedure gave slight irregularities (maximum 5%) in the density dependence of the entropy at 3.5 K, our top temperature of integration, which we averaged by drawing a smooth curve through the 3.5-K results. Using the smoother 3.5-K entropies as reference we constructed entropy-density isotherms, portions of which are shown in Fig. 11. Given the rather spaced coverages we had measured and the entropy averaging above, we did not draw isotherms any closer than 0.04 K (or 0.014 for $|t|$). From a digitized version of a graph such as Fig. 11 we numerically calculated μ from 3.5 K down. We used for μ(3.5 K) values calculated for ^{4}He/Grafoil by Elgin in Ref. 23. These values are not exactly the same as for our foam substrate since substrate effects are included in μ, but although the magnitude of μ may vary slightly, its density dependence at 3.5 K should be close to the one of Grafoil, particularly over the limited range of densities used here.

From the calculated μ-T(constant n) table, paths of constant μ were determined. Three of these paths are shown in Fig. 9; the $\mu/k_B = -139.60$ K line is also shown in Fig. 11. It is along this path that the C_μ of Fig. 10 has been calculated. One can see that the constant path approaches the critical line with a slope closer to the entropy isotherm slopes than the constant-n path with about the same critical temperature. This leads to a higher C_μ than C_n, and in fact if the constant-μ path came exactly parallel (in an ideal system) to $S(T_c)$, C_μ would diverge to infinity.

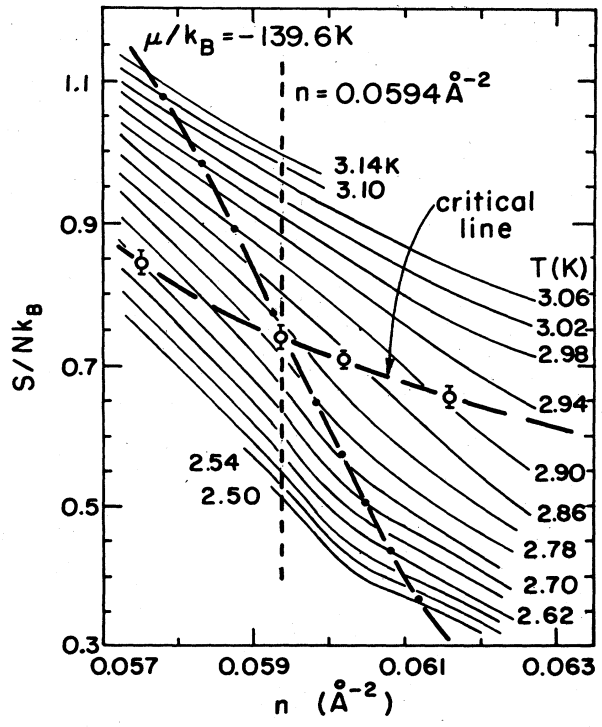

FIG. 11. Entropy-density (constant-T) lines for ^{4}He/graphite in our calorimeter. The constant-density and constant-chemical-potential paths shown are the ones along which the measured and calculated specific heats of Fig. 9 were obtained.

The following qualitative argument also accounts for the change in peak amplitude (decrease) with increasing x. In the crossover region, the heat-capacity behavior will change from $A|t|^{-\alpha}+B$ to $D-G|t|^{-\alpha_R}$. A, B, D, and G are nonsingular functions of T, being approximately constant very near the critical temperature. D determines the maximum height of the renormalized heat capacity. If we approximate that at crossover $t=t_{cr}$ and $At_{cr}^{-1/3}+B=D-Gt_{cr}^{1/2}$, since $t_{cr}\sim x^{1/\alpha}=x^3$ for small x and A and B are essentially independent of x as shown in Fig. 8, we obtain $D\sim 1/x$. This dependence is semiquantitatively followed by the peaks amplitude, except extremely close to n_c (the peak at the perfect commensurate density is finite, not infinite). It cannot be verified accurately because of the approximations made in the theoretical estimate and the experimentally rounded (rather than cusped) specific heat.

Given the approximations made on calculating C_μ, we have not attempted to calculate α for the C_μ of Fig. 10. A more detailed and extensive set of data, including an accurate reference chemical potential, is necessary for such an analysis. We are now attempting to obtain such a set of data.

We also produced an entropy-density course set of isotherms around the TCP. Constant-μ paths were determined as described above, but in this case we used Elgin's 3.0-K chemical-potential table for the reference μ. Elgin's table at this temperature is considerably coarser than the detailed 3.5-K data used for the critical-line study. In addition, μ varies very weakly with temperature at these densities, so tracking the constant-μ line is very difficult and results are only qualitatively correct. Figure 12 shows the result of this calculation as (S/Nk)-versus-n(constant T) plots. We included in Fig. 6 the two constant μ/k_B lines (-142.3 and -144.0 K) of Fig. 12. The most interesting conclusion to be drawn from these lines of constant μ is that they will again lead to strongly diverging constant-μ specific heats. This is particularly revealing since at the TCP C_h does not diverge [see Eq. (2)], but for the 2D three-state Potts system, C_μ should diverge with $\alpha=\frac{5}{6}$, a very strong divergence. This appears to be the case for our system. Unfortunately no quantitative calculations can be done without a very accurate and fine grid set of heat-capacity and vapor-pressure measurements to construct a good entropy-density-temperature table and obtain $\mu(T)$. In addition, heterogeneities may be much more important at the TCP judging by the width of the first-order peaks at the two-phase boundary.

Heterogeneities plague all of the surface experiments done on systems such as the one of this study. Although

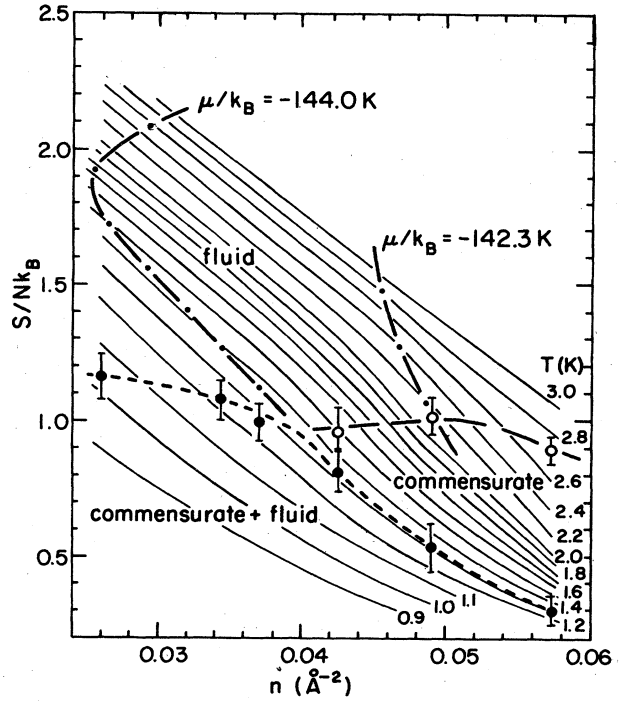

FIG. 12. Entropy-density (constant-T) lines for ^{4}He/graphite in our calorimeter. Diagram shows the critical line (——) and two phase region boundaries (— — —), as well as two qualitative constant-chemical-potential paths. The one at $\mu/k_B = -144.0$ K approximately corresponds to a line across the TCP.

estimates of the effect of substrate energy variations and finite size have been included in several previous publications (Novaco,[15] for example, calculated the effects of variations in substrate binding energy for a simple thermodynamic model of ^{4}He and found quantitative agreement with Grafoil experimental data), a detailed study of their effect on various phases and types of measurements dates to recent efforts of Dash and Puff,[36] and Ecke, Dash, and Puff[16] who laid the foundation for a theoretical understanding of the problem and proceeded to calculate a model van der Waals system with certain types of heterogeneities. More recently, Ecke and Dash[28] studied experimentally the systems Xe/graphite and ^{4}He/graphite using a foam substrate like the one used in this experiment. On the basis of this last study we have estimated the expected temperature widths for the low-density peaks ($n < n_{\mathrm{TCP}}$). The temperature width is given approximately by

$$\delta T \cong \frac{dT}{dn} n^2 K_T \delta\epsilon \,, \tag{3}$$

where dT/dn is the phase-boundary slope, K_T is the isothermal compressibility of the condensed phase, and $\delta\epsilon$ is the variation in substrate binding energy. We obtained K_T from Elgin and Goodstein's thermodynamic analysis of ^{4}He/Grafoil.[22] The variation in substrate binding for ^{4}He/foam is taken to be $\delta\epsilon = 0.1$ K from Ref. 15. Redistribution effects[16,28] will increase the rounding over the estimate given by Eq. (3) by about a factor of 3. We obtain a temperature width of 0.3 K, in agreement with Novaco's calculation and with the experimental data. Although the low-density peaks of the graphite-foam data are 15% to 20% greater in magnitude than the Grafoil peaks at comparable densities and the domain size is at least several times larger for graphite foam,[9,28] the temperature rounding is virtually identical. This implies that variations in substrate binding energy, as opposed to a finite-size mechanism, dominate the rounding of the low-temperature specific-heat peaks and that the energy variation for graphite foam and Grafoil are about the same.

Along the critical line, on the other hand, the temperature rounding, as measured by the inflection points of the peak, decreases with increasing density. Estimates of the rounding due to binding energy variations using Eq. (3) and our own chemical-potential data, are at least a factor of three smaller than the experimental widths in regions of high slope in the phase boundary, and even smaller closer to n_c. Also the specific-heat peak maxima at n_c vary by 50% to 100% for different graphite substrates, while the low-density peaks (and the high-density melting peaks of Ref. 28 measured on a similar substrate) only vary by 15% to 20%. This suggests that along the critical line finite size is the important mechanism for peak rounding.

V. SUMMARY

We have found specific-heat peaks which delineate the two-phase coexistence region and the lower boundary of the registered-phase region of ^{4}He adsorbed on graphite. We tentatively locate the tricritical point at $n_{\mathrm{TCP}} \cong 0.039$ Å^{-2} and $T_{\mathrm{TCP}} \cong 1.3$ K although the possibility of a narrow coexistence region with a tricritical point at somewhat higher temperature and density is also consistent with the experimental data. In the vicinity of the critical coverage, we observe specific-heat peaks which seem to show evidence of Fisher renormalization. Specifically, a reconstructed constant-chemical-potential specific-heat peak at $n = 0.0593$ Å^{-2} is very similar in height and shape to the specific heat at the exactly commensurate density. We identify regions where respectively critical, renormalization, and finite-size behavior dominate the specific heat.

ACKNOWLEDGMENTS

The authors acknowledge the help and advice of M. Schick and P. Nightingale, and in particular M. den Nijs, J. J. Rehr, and E. K. Riedel, who spent many hours with the authors reviewing the properties of the 2D three-state Potts model and Fisher renormalization, and J. G. Dash, who made many relevant comments during the experimental run and during the writing of this manuscript. One of us (O.E.V.) acknowledges a helpful discussion regarding renormalized critical exponents with A. N. Berker. We thank Christine Platt for help during the final run. This work was supported by the National Science Foundation under Grant Nos. DMR-81-16421 and DMR-80-22239.

*Present address: Los Alamos National Laboratory, P10-K764, Los Alamos, New Mexico 87545.

†On leave from Low Temperature Division, Department of Thermal Physics, Zhejiang University, China. Present address: Department of Physics, Queen's University, Kingston, Canada K7L 3N6.

[1]M. Bretz, J. G. Dash, D. C. Hickernell, E. O. McLean, and O. E. Vilches, Phys. Rev. A **8**, 1589 (1973).

[2]M. Nielsen, J. P. McTague, and W. Ellenson, J. Phys. (Paris) Colloq. **38**, C4-10 (1977).

[3]H. J. Lauter, H. Wiechert, and R. Feile, in *Ordering in Two Dimensions,* edited by S. K. Sinha (North-Holland, New York, 1980), p. 291.

[4]S. Alexander, Phys. Lett. **54A**, 353 (1975).

[5]Grafoil, *ZYX*, and graphite foam are various forms of exfoliated graphite marketed by the Union Carbide Corporation.

[6]M. Bretz, Phys. Rev. Lett. **38**, 501 (1977).

[7]M. den Nijs, J. Phys. A **12**, 1857 (1979).

[8]R. J. Baxter, J. Phys. A **13**, L61 (1980).

[9]M. J. Tejwani, O. Ferreira, and O. E. Vilches, Phys. Rev. Lett. **44**, 152 (1980).

[10]S. B. Crary and D. A. Fahey (unpublished). This article contains, in addition to their own measurements, a comprehensive comparison of all previous data of Refs. 1, 6, and 7. We thank Dr. Crary for making the results of this article available to us previous to its submission. D. A. Fahey, B.S. dissertation, Amherst College, 1982.

[11]R. L. Siddon and M. Schick, Phys. Rev. A **9**, 907 (1974); **9**, 1753 (1974).

[12]A. D. Novaco, Phys. Rev. A **7**, 1653 (1973).

[13]M. W. Cole and D. R. Frankl, Surf. Sci. **70**, 585 (1978); W. E. Carlos and M. W. Cole, Phys. Rev. B **21**, 3713 (1980).

[14]D. E. Hagen, A. D. Novaco, and F. J. Milford, in *Adsorption-Desorption Phenomena,* edited by F. Ricca (Academic, New York, 1972), p. 99.

[15]A. D. Novaco, J. Low Temp. Phys. **9**, 457 (1972).

[16]R. E. Ecke, J. G. Dash, and R. D. Puff, Phys. Rev. B **26**, 1288 (1982).

[17]M. Schick, J. S. Walker, and M. Wortis, Phys. Rev. B **16**, 2205 (1977).

[18]A. N. Berker, in *Ordering in Two Dimensions,* edited by S. K. Sinha (North-Holland, New York, 1980) p. 3.

[19]B. Nienhuis, A. N. Berker, E. K. Riedel, and M. Schick, Phys. Rev. Lett. **43**, 737 (1979).

[20]M. den Nijs (private communication). We greatly benefited from a series of lectures by Professor den Nijs. All values of the critical exponents quoted in this paper were obtained from his lecture notes.

[21]E. K. Riedel, H. Meyer, and R. P. Behringer, J. Low Temp. Phys. **22**, 369 (1976). The analysis of the thermodynamics of ^{3}He-^{4}He mixtures is somewhat analogous to the study of the ^{4}He/graphite system.

[22]R. L. Elgin and D. L. Goodstein, Phys. Rev. A **9**, 2657 (1974).

[23]R. L. Elgin, Ph.D. dissertation, California Insitute of Technology, 1973.

[24]R. L. Elgin, J. M. Greif, and D. L. Goodstein, Phys. Rev. Lett. **41**, 1723 (1978).

[25]M. E. Fisher, Phys. Rev. **176**, 257 (1968).

[26]Cryo-Cal, 2457 University Avenue, St. Paul, MN 55114.

[27]Model 330 SQUID system, S.H.E. Corporation, 4174 Sorrento Valley Blvd., San Diego, CA 92121.

[28]R. E. Ecke, Ph.D. dissertation, University of Washington, 1982; R. E. Ecke and J. G. Dash, Phys. Rev. B **28**, 3738 (1983).

[29]M. Bienfait, J. G. Dash, and J. Stoltenberg, Phys. Rev. B **21**, 2765 (1980).

[30]D. M. Butler, J. A. Litzinger, G. A. Stewart, and R. B. Griffiths, Phys. Rev. Lett. **42**, 1289 (1979).

[31]A. D. Migone, M. H. W. Chan, K. J. Niskanen, and R. B. Griffiths, J. Phys. C **16**, L1115 (1983).

[32]B. J. Lipa and M. J. Buckingham, Phys. Lett. **26A**, 643 (1968).

[33]M. E. Fisher and P. E. Scesney, Phys. Rev. A **2**, 825 (1970).

[34]E. K. Riedel and F. J. Wegner, Phys. Rev. B **9**, 294 (1974).

[35]D. C. Hickernell, E. O. McLean, and O. E. Vilches, J. Low Temp. Phys. **23**, 143 (1974).

[36]J. G. Dash and R. D. Puff, Phys. Rev. B **24**, 295 (1981).